Proceedings of the 17th World Congress
The International Federation of Automatic Control
Seoul, Korea, July 6-11, 2008

Image Processing and Roughness Analysis as a Tool for Quantification of Physiological Well-Being in plants: Results for Sunagoke Moss

S. Ondimu*, H Murase*

* Bio-instrumentation, Control and Systems (BICS) Engineering Lab., School of Life and environmental Sciences, Osaka Prefecture University, 1-1, Gakuen-cho, Sakai City, Osaka. Japan. Zip: 599-8531. Corresponding author: Stephen Ondimu:- phone: 81-72-254-9429; fax: 81-72-254-9918; e-mail: Ondimu@bics.envi.osakafu-u.ac.jp

Abstract: The general appearance of a plant is the most obvious indicator of its physiological well-being. This study was premised on the assumption that image roughness values can be used to quantify well-being in plants. We hypothesize that the highest level of well-being in the plant corresponds to a given minimum level of its surface roughness. Beyond this point the roughness increases. A set of 511 images of Sunagoke moss (Rhacomitrium canescens) samples at water states of, $5.0gg^{-1}$, $4gg^{-1}$, $3gg^{-1}$, $2.0gg^{-1}$, $1.0gg^{-1}$ and $0gg^{-1}$ were analyzed for roughness parameters. Water state here was defined as the amount of water available for the plant at the beginning of a given day in grams per gram of its dry weight. The results demonstrated that different water states have a strong effect on the surface roughness in Sunagoke moss. It was found that the higher the surface roughness of a plant the lower the level of its well-being and vice-versa. The highest level of well-being was found to be at $2gg^{-1}$ water state for the Sunagoke moss used in this study. We concluded that roughness analysis can be used to quantify well-being in plants. Based on the results of this study, we propose a speaking organism system concept which allows plants to self-regulate their own bio-production environment based on roughness parameters fused with other image analysis results.

1. INTRODUCTION

The general appearance of plants is the most obvious indicator of their physiological well-being. For this reason, imaging techniques are emerging as novel techniques for non destructive detection of physiological state in plants. These techniques make real-time monitoring and analysis of physiological changes in plants, often characterized by a lot of dynamics and non-linearity (Hall & Lima, 2001) possible. Some of the imaging techniques applied in plants include fluorescence imaging, bioluminescence imaging, thermal imaging, magnetic resonance imaging and reflectance imaging (Chaerle *et al.,* 2001).

Plant well-being is influenced by physiological stress. Plant stress is an external factor that exerts a disadvantageous influence on the plant (Taiz & Zeiger, 2002). Response to stress is expressed at gene (DNA), cellular, organ and whole organism levels in plants. Stress in plants influences stomatal resistance, induces changes in surface and internal leaf structure, causes accumulation of metabolites or leads to the break down of photosynthetic pigments (Peñuela & Filella, 1998). Internal responses to these changes in a plant are reflected on its surface structure and transpiration patterns in form of its top projected canopy area (TPCA), canopy temperature or multispectral reflectance. Structural alterations modify reflection of light from plant leaves or canopies. Factors leading to a decrease in light absorption automatically increase reflection and vice versa. These changes can be visualised by reflectance imaging either in the visible or near-infrared spectrums and can be used to indicate well-being in plants.

Visual imaging of plant canopies can provide indirect data which can be used to derive their structural or functional changes (Peñuelas & Filella, 1998) and has been widely used in detecting and quantifying physiological changes and accompanying biotic and abiotic stressors in plants (Kacira *et. al*., 2002; Carter & Miller, 1994; Kacira & Ling, 2001; Foucher *et.al.,* 2004; Ceccato *et al.,* 2001; Mirik *et al.,* 2006; Díaz-Lago *et al*., 2003). Most of these investigations use either grey-level textural features or color information based on the Red-Green-Blue (RGB) model. However, relatively little is known about the relationship between color information and textural attributes (Yin and Panigrahi, 2004). In addition, grey-level texture features tend to be globally adaptable but they are not locally optimized.

This study is based on the premise that image roughness analysis is more friendly and closer to the human perception of surfaces. Roughness analysis has been applied in materials development and failure analysis, precision component machining, corrosion analysis, paper production and medical device development. In biological systems, many studies have shown an inherent link between surface roughness well-being (Anderson *et al*., 2006; Chung *et al*., 2003; Tomovich and Peng, 2005; Yang *et al.,* 2005; Yonekana *et al.,* 1996).

There are numerous methods of establishing surface roughness. Optical methods involve use of microscopes, optical profilers and scattermetry. Electron or ion beam methods rely on differing emission of electrons to establish the roughness of a surface.

Mechanical profilers rely on a mechanical stylus that traces the roughness profile of a given surface. All these methods have their advantages and disadvantages. However, they are generally limited in scale and thus may not effectively be used for biological systems. In this study, a method that allows extraction of roughness parameters from visual reflectance images was used. Roughness parameters were extracted and used to quantify water stress in Sunagoke moss. The study was based on the fact that Sunagoke moss has the same chlorophyll-protein complexes as high plants (Aro *et al.,* 1981) and alterations in its chlorophyll absorption induce changes in its surface and internal leaf structure which modify reflection of light from its canopy. These changes can be visualized by reflectance imaging, and thus be used to quantify its well-being.

1.1 Surface Roughness Analysis

Roughness analysis mainly entails determination of roughness parameters of a given surface. Roughness parameters are statistical parameters that measure the vertical characteristics of the surface. Roughness analysis of 2D optical colour images mainly entails: image pre-processing, multi-resolution filtering and roughness parameter determination. Here is a brief description of the roughness parameters used in this study:

1. **Arithmetical mean deviation (Ra):** This is the average roughness deviation of all points from a plane to the test part surface. It is obtained by:

$$R_a = \frac{1}{n_x n_y} \sum_{i=1}^{n_x} \sum_{j=1}^{n_y} \left| Z(i,j) - Z_{ave} \right| \qquad (1)$$

where, Z (i,j) denotes the topography data for the surface after image tilt-correction (surface-levelling), Z_{ave} average surface height, i and j corresponded to the pixels intensities in the x and y direction and n_x and n_y maximum number of pixels in the x and y directions (Lindset and Bardal, 1999). In this study, tilt-correction was achieved by scanning the surface profile and calculating the surface plane according to Bhattacharyya and Johnson (1997) using (2).

$$z_i = z_i(\alpha + \beta_1 x_{i1} - \beta_2 x_{i2}) \qquad (2)$$

where, z_i is surface profile, β_1, β_2 are regression coefficients (weights), α is a constant when both variable are zero and x_{i1} and x_{i2} are pixel values. The term in the brackets is the regression plane.

2. Root mean square (rms) deviation (Rq): The average of the measured height deviations taken within the evaluation of length or area and measured from the mean linear surface. It is given by:

$$R_q = \left[\frac{\sum_{i=1}^{n_x} \sum_{i=j}^{n_y} [Z(i,j) - Z_{ave}]^2}{n_x n_y} \right]^{\frac{1}{2}} \qquad (3)$$

3. Lowest valley (Rv): This is the maximum distance between the mean line and lowest point within the sample. It is the maximum data point height below the mean line through the entire data set.

4. Highest peak (Rp): This is the maximum distance between the mean line and the highest point within the sample. It is maximum data point height above a mean line through the entire data set.

5.0 The total height of the profile (Rt): The absolute value between the highest and lowest peaks. It was computed using (4).

$$R_t = R_p + R_v \qquad (4)$$

6. Surface area, given in calibrated units (SA): This is the surface area of the roughness profile

This study is based on the premise that the magnitude of surface roughness parameters in a plant can be used to quantify its well-being. We hypothesize that the highest level of well-being in a plant corresponds to a given minimum level of its surface roughness. Beyond this level, roughness increases. This implies that the higher the magnitude of surface roughness parameters the lower the level of well-being in a plant and vice-versa.

1.2 Goal and Objectives

The overall aim of this study is to develop a stress-imaging system that utilizes surface roughness parameters to monitor physiological well-being in plants. The objectives were to:

- compute surface roughness parameters from images of Sunagoke moss under different daily water states
- evaluate the correlation between the parameters obtained the previous objective and well-being in the sample.
- propose a speaking organism system concept that allows plants to self-regulate their environment via quantification of their well-being by image analysis

2. MATERIAL AND METHODS

2.1 Sunagoke moss sample

Figure 1 shows one of the Sunagoke moss (Rhacomitrium canescens) samples used in this study. Nine similar samples were used in total. The samples were subjected to different water states as a means of manipulating its well-being. Water state here was defined as the amount of water available to the sample at beginning of each day of data acquisition in grams per gram of its dry weight. The water sates used in this study were: $5gg^{-1}$, $4gg^{-1}$, $3gg^{-1}$, $2gg^{-1}$, $1gg^{-1}$, and 0. Images were acquired for five consecutive days for each water state. At the start of each day of experiment, the water state of each sample was computed and replenished accordingly. A two day interval was allowed between each experiment. It should

be noted here that Sunagoke moss exhibits a high level of desiccation tolerance (Aro et al., 1981; Bowen, 1933; Valanne, 1984). It suspends its photosynthesis and transpiration when dry only to resume biological activity when exposed to moisture. This made it possible to use the same samples throughout the study to avoid errors due to natural discrepancies inherent in biological systems. To introduce some randomness to the image data, the order of data acquisition was: $5gg^{-1}$, $3gg^{-1}$, $2gg^{-1}$, $4gg^{-1}$, $1gg^{-1}$ and 0.

Fig. 1 Sunagoke moss sample used in this study

2.2 Experimental data acquisition system

The procedure used in determining roughness parameters was as summarized in Fig. 2. RGB images of size 480×640 pixels were acquired with a CCD video camera, TRV22E (Sony corporation, Japan) placed at 300 mm perpendicular to the sample surface as shown in Fig.3. Images were acquired after every 10 minutes giving 73 images per day of experiment. Light was provided by two 22W lamps (EFD25EN/22, National Corporation, Japan) giving an average of intensity of 82.32 $\mu mols^{-1}$ or 7.20 *Klux* (400-700 nm) inside the growth chamber (measured by Li-250A- light meter; Li-COR, USA). Data acquisition was conducted in a walk-in growth chamber (NK-system) with temperature and humidity set to 15 oC and 60% respectively. The light/dark period was 12 hours. After acquisition, ImageJ ver 3.8 (Rasband, NIH) software was used for processing and analyzing the images. Images acquired on the third day for each water state were selected for roughness analysis giving a total of 511 images. It was assumed that by this day the sample had acclimatized well to the prevailing water state.

2.3 Image processing and roughness parameter extraction

First the RGB images were resized to 292 × 400 pixel by cropping. After histogram equalization, they were converted to 32 bit floating point grey-level images to reveal more details in the shadows than in the highlights (in line with human vision). Tilt correction was then carried out using (2). After a number of trials, a sampling length of 5 pixels was selected for local sampling to ensure that roughness statistics are accessed on local regions according to the given sampling length. The reported roughness values per sample are the average of all the roughness in the local sub-images.

A gradient analysis was performed on the images to calculate SA prior to the determination of roughness parameters (R-values). Two filtering routines: Gaussian filtering (GF) and Fast Fourier Transform (FFT) bandpass filtering were used to decompose the processed images into roughness images (high frequency information) and waviness images (low frequency information). The GF radius was 5 pixels and the FFT bandpass filter size was 10 × 20 pixels.

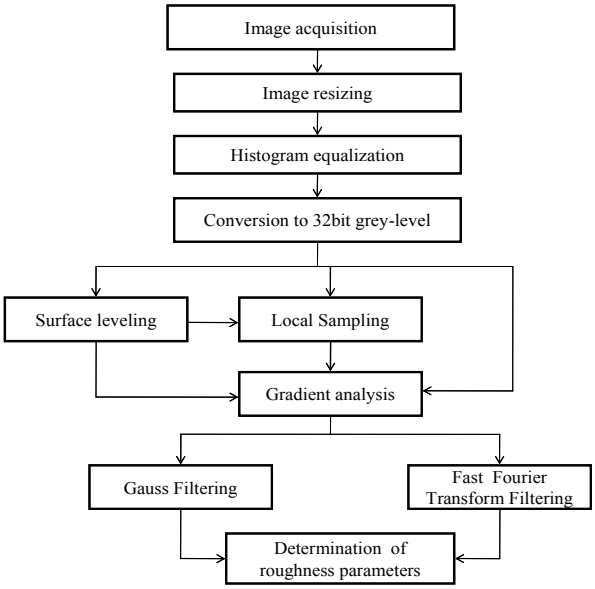

Fig. 2. Process for determining surface roughness statistics

Fig. 3. Image acquisition system

2.4 Excess green well-being index

An excess well-being index (EGWI) was determined using (5) to quantify well-being in the samples. The EGWI is premised on the assumption that the greener the plant the higher the quality of its well-being and vice-versa.

$$EGWI = \frac{AG_EI - AG_EI_U}{AG_EI_L - AG_EI_U} \quad (5)$$

$$AG_EI = \frac{2G-R-B}{N} \quad (6)$$

where: NG_EI = average excess green index given by (6); AG_EI_U = average excess green index of a non-respiring plant (upper limit); AG_EI_L= average excess green index of a non-stressed plant (lower limit); R, G and B are the pixel intensity values for the red, green and blue channels and N is the total number of pixels in the image.

3.0 RESULTS AND DISCUSSION

Figure 4 shows three-dimensional profiles of roughness images of one of the Sunagoke moss samples at different water states. Average roughness parameters extracted from similar profiles for the nine samples are listed in Table 1.

Table 1. Average roughness parameters of Sunagoke moss at different water states: (a) Gauss Filtering (GF); (b) Fast Fourier Transform (FFT) band pass filtering

Water state (gg^{-1})	Roughness Parameters					
	Rq	Rv	Rv	Rp	Rt	SA
5	31.45	-61.97	-61.97	61.49	123.46	1752340.31
4	26.18	-53.78	-53.78	51.20	104.98	1340797.40
3	25.92	-53.55	-53.55	46.86	103.94	1347291.47
2	25.02	-52.86	-52.86	58.60	99.72	1263466.20
1	31.44	-62.24	-62.24	58.60	120.84	1836483.86
0	39.62	-78.12	-78.12	75.01	145.13	2258519.21

(a)

Water state (gg^{-1})	Roughness Parameters					
	Rq	Ra	Rv	Rp	Rt	SA
5	1.35	1.11	-2.28	2.44	4.72	1752340.31
4	1.25	1.03	-2.97	2.39	4.36	1340797.40
3	1.19	0.99	-2.01	2.17	4.18	1347291.47
2	1.16	0.96	-1.84	2.22	4.06	1263466.20
1	1.87	1.54	-3.12	3.42	6.53	1836483.86
0	2.54	2.10	-4.44	4.45	8.90	2258519.21

(b)

The minimum values of Rq, Ra, Rt, Rp and Sa coincided with the maximum values of Rv at $2gg^{-1}$ water state. On either side of this water state, the values of these parameters conversely increased or decreased, respectively. This is more clearly shown in Figs 5 and 6. This is more distinctly illustrated by Fig. 5. This implies that the well-being of the sample was highest at a $2gg^{-1}$ water state. EGWI values computed using (5) were 0.76, 0.67, 0.86, 0.55, 0.27 and 0.13 for $5gg^{-1}$, $4gg^{-1}$, $3gg^{-1}$, $2gg^{-1}$ and $0gg^{-1}$ water states, respectively. High EGWI values depict high well-being and vice-versa. In this regard, the highest well-being depicted by the EGWI was at $3gg^{-1}$ compared to $2gg^{-1}$ for roughness parameters. This was attributed to the fact that changes in light absorption (espoused by EGWI) precede changes in surface structure (espoused by R-values) in plants. Hence, EGWI can detect changes in plant well-being before such changes become apparent to humans.

Table 2 shows the standard deviations of the roughness values listed in Table 1. Roughness values at $1gg^{-1}$ water state displayed the highest variation.

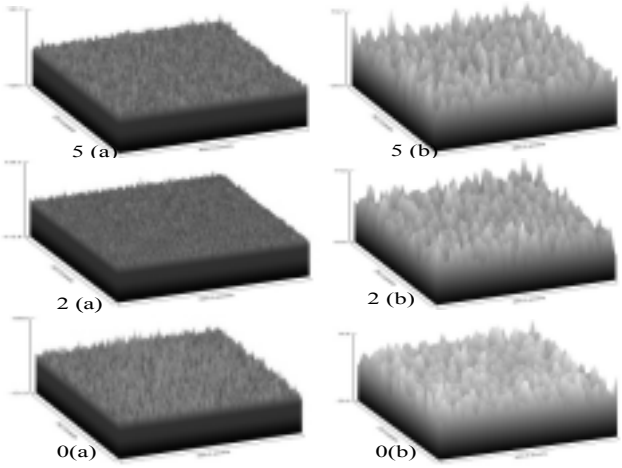

Fig. 4. Samples of three-dimensional profiles of roughness images of Sunagoke moss at different water states: (a) Gaussian Filter (GF); (b) FFT bandpass filter. The numbers 5, 2 and 0 represent water states in gg^{-1}

Table 2 Standard deviation roughness parameters of Sunagoke moss at different water states: (a) Gauss Filtering (GF); (b) FFT bandpass filtering

Water state (gg^{-1})	Standard deviations of roughness parameters					
	Rq	Ra	Rv	Rp	Rt	SA
5	2.33	1.85	4.08	4.75	8.81	188814.07
4	1.14	0.87	2.30	2.27	4.55	90522.59
3	1.71	1.31	3.48	3.48	6.93	38672.42
2	1.15	0.89	2.73	1.96	4.59	91060.93
1	7.55	6.41	9.24	15.34	24.53	65141.74
0	1.22	1.00	1.84	2.43	4.20	101634.72

(a)

Water state (gg^{-1})	Roughness Parameters					
	Rq	Ra	Rv	Rp	Rt	SA
5	0.05	0.04	0.10	0.08	0.18	3230.66
4	0.03	0.02	0.08	0.08	0.10	1744.42
3	0.02	0.02	0.06	0.04	0.08	1350.24
2	0.07	0.06	0.20	0.09	0.26	4449.42
1	0.70	0.58	1.38	1.12	2.43	48312.34
0	0.06	0.05	0.11	0.11	0.20	4217.27

(b)

This is because at this water state, the samples initially had enough water to meet their net fixation. But this was depleted quickly due to evapotranspiration exposing the samples to extreme water deficit. This caused the roughness values to vary from low to high in the same day.

Figure 5 shows the effect of sampling and levelling (tilt-correction) on Ra and Rq values in Sunagoke moss. The results in Fig. (5a and 5b) show that local sampling has great

influence on Ra and Rq values. On the other hand, tilt-correction has no significant effect on the magnitude of the same parameters. We made similar observations for the other roughness parameters shown in Table 1.

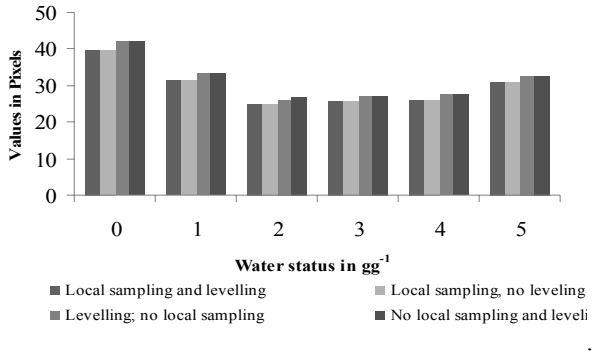

(a)

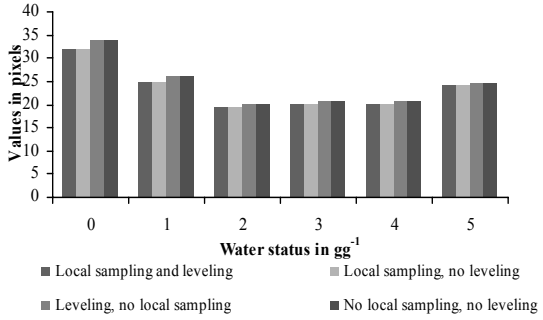

(b)

Fig. 5. Effect sampling and tilt-correction on roughness parameters: (a) average Rq values (b) average Ra values

The relationship between Ra and Rq values for Sunagoke moss at different water states is shown in (Fig. 6). The results show that Ra varied with Rq with a linear relationship of 0.84 and 0.78 for values obtained by GF and FFT bandpass respectively.

Figure 7 shows average values of (RSurfAreaRatio) i.e. the ratio between SA of roughness images and SA of the original images for the samples used in the study.These results show that different water states have a strong effect on surface roughness in Sunagoke moss. Thus roughness values can be used to quantify its well-being. Lower roughness values depict a higher degree of well-being and vice-versa.

CONCLUSIONS

In this study image processing and roughness analysis was used to quantify well-being in Sunagoke moss. Roughness parameters of nine samples at different water states were analysed. The results obtained showed that well-being, in Sunagoke moss was highest only at a particular water state ($2gg^{-1}$). A above or below this water state, surface roughness increased, indicating deterioration of well-being. Though Sunagoke moss was used in this study, these results can be extended to other plants.

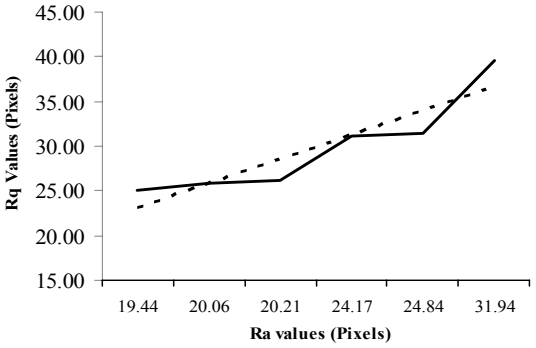

(a)

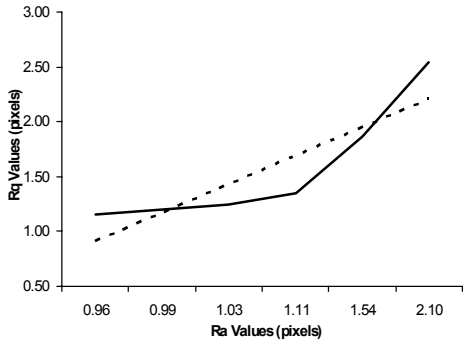

(b)

Fig. 6. Correlation between Ra and Rq values of Sunagoke moss (pixels) analyzed by visual imaging, the dotted lines are trend lines: (a) via Gauss Filter (GF); y=3.339x + 16.07, R2 = 0.936; (b) via FFT Bandpass filter; y = 0.386x + 0.635, R^2 = 0.908

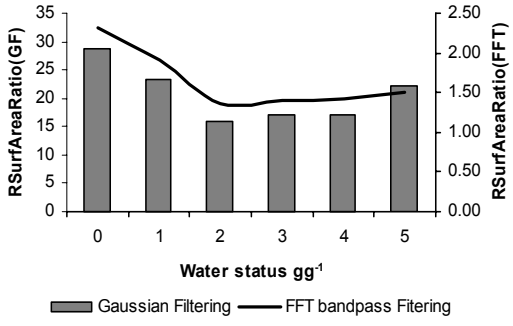

Fig 7. RSurfAreaRatio values of Sunagoke moss analyzed by visual imaging

We propose that roughness analysis can be used to develop a speaking organism system that allows plants to control their own bio-production environment. Fusing roughness results with other image analysis results will make such a system even more robust. A system that allows plants to self-control their own bio-production environment will be a great and

timely boost for high value plants especially those of medicinal and vaccine value in which the bio-production environment critically influences their effectiveness. The concept of such a system is illustrated in the appendix.

REFERENCES:

Anderson, K. R., Anderson, E., Shakir, L. and Glover, C. G. (2006). Image analysis of Extracellular Matrix Topography of Colon Cancer Cells. Microscopy and Analysis 20(4):5-7 (UK).

Aro E M, Niemi H. and Valanne N. (1981). Structural and functional studies on bryophyte phptonsythesis. In "Photonsythesis" (G Akoyunoglou, ed.) 3 : 327-335. Balaban Int. Sci. Serv., Philadelphia, Pennesylvannia.

Bhattacharyya, A., Johnston (1997). Statistics: Principles and Methods (3rd edition). Weley.

Bowen, E. J. (1933). The mechanism of water conduction in Musci considered in relation to habitat. II. Mosses growing in dry environments. Annals of Botany (London) 47: 889-912.

Carter, A. G. and L. R. Miller (1994). Early detection of plant Stress by digital imaging within narrow stress-sensitive wavebands. Remote Sensing Environment (50): 295-302.

Ceccato, P., S. Flasse, S.Tarantola, S. Jacquemound and J. Grègoire. (2001). Detecting vegetation water content using reflectance in the optical domain. Remote Sensing of Environment, 77: 22-33.

Chaerle, L. and D. Van Der Straeten. (2001). Seeing is believing: imaging techniques to monitor plant health. Biochimica et Biophysica Acta 1519 :153-166.

Chinga, G., Johnssen, P. O., Dougherty, R., Lunden-Berli, E. and Walter J. (2007). Quantification of the 3-D micro-structure of SC surfaces. Journal of Microscopy 227(3): 254-265.

Chung, T. W., Liu, D. Z., Wang, S. S. and Wang, S. Y. (2003). Enhancement of the growth of human endothelial cells by surface roughness at nanometer scale. Biomaterials 24(25) 4655-4661.

Curray, J. R. (1956). The analysis of two orientation data. Journal of Geology, 64: 117-131.

Díaz-Lago; J. E., D. D. Stuthman, K. J Leornard. 2003. Evaluation of componetnts of partial resistance to oat crown using digital image analysis. Plant Disease, 87: 667-674.

Foucher, P., P. Revollo, B. Vigouroux and G Chassériaux (2004). Morphological image analysis for the detection of water stress in potted Forsythia. Biosystems Engineering 89(2): 131-138.

Hall, S. G. and Lima, M. (2001). Problem-Solving Approaches and Philosophies in Biological Engineering: Challenges from technical, social, and ethical arenas. Transactions of ASAE 44 (4): 1037-1041.

Kacira, M., P. P. Ling and T. H. Short. (2002). Machine vision extracted plant movement for early detection of plant water stress. Transactions of ASAE 45(4): 1147-1153.

Kacira, M. and P. P. Ling (2001). Design and development of an automated and Non–contact sensing system for continuous monitoring of plant health and growth. Transaction of ASAE 44(4): 989-996.

Lindset, I. and Bardal, A. (1999). Quantitative topography measurements of rolled aluminium surfaces by atomic force microscopy and optical methods. Surface and coatings technology, 111:276-286.

Mirk, M., G. J. Michels Jr., S. Kassymzhanova-Miril, N. C Ellio, V. Catana, D. B. Jones and R. Bowling. (2006). Using digital image analysis and spectral reflectance data to quantify damage by Greenburg (hemitera: Aphididae in winter and wheat. Computers and Electronics in Agriculture 51:86-98.

Peñuelas, J. and I. Filella, (1998). Visible and near-infrared reflectance techniques for diagnosing plant physiological status. Trends in Plant Science 3: 151-156.

Rasband, W. (2007). ImageJ 1.38r. National Institute of Health (NIH) USA. Available at: http://rsb.info.hih.gov/ij/.

Taiz L and Zeiger E (2002). Plant Physiology. Sinauer Assocites Inc., Sunderland, MA, USA.

Tomovich, S. J. and Peng, Z. (2005). Optmised reflection imaging for surface roughness analysis using confocal scanning microscopy and height encoded image processing. Journal of Physics: Conference series 13: 426 – 429.

Valanne, N. (1984). Photonsythesis and Photonsythetic Products in Mosses. In The Experimental Biology of Bryophytes (ed. by Dyer, A. J., Duckett , J. G), Academic press, London, 257-273.

Yang, H., An, H., Feng, G. and Li, Y. (2005). Visualization and quantitave roughness analysis of peach skin by atomic force microscopy under storage. LWT 38 271 -577. Available on-line: www.sciencedirect.com Yin, H., Panigrahi, S. (2004). Image processing techniques for internal texture evaluation of French Fries. Applied Engineering in Agricultur. 20(6): 803-811.

Yonekawa, S. Sakai, N. and Kitani, O. (1996). Identification of idealized leaf types using simple dimensionless shape factors by image analysis. Transaction of ASAE 39(4) 1525-1533: ISSN 0001-2351.

Appendix: Schematic of concept of speaking organism system that allows plants to self-regulate their own environment